

## Supporting Information

### Inorganic $\text{Cu}_2\text{ZnSnS}_4$ Hole transport layer for Perovskite Light-Emitting Diodes

Lunyao Pan,<sup>a</sup> Wen Li,<sup>\*a</sup> Xiankan Zeng,<sup>a</sup> Maolin Mu,<sup>a</sup> Qungui Wang,<sup>b</sup> Yongjian Chen,<sup>a</sup> Chenglong Li,<sup>a</sup> Shiyu Yang,<sup>a</sup> Linzhu Dai,<sup>c</sup> Li Tao,<sup>d</sup> Weiqing Yang<sup>\*ac</sup>

a. Key Laboratory of Advanced Technologies of Materials (Ministry of Education), School of Materials Science and Engineering, Southwest Jiaotong University, Chengdu 610031, PR China.

b. College of Physics, Sichuan University, Chengdu 610065, PR China.

c. School of Chemistry and Chemical Engineering, Southwest University, Chongqing 400715, PR China.

d. School of Optoelectronic Engineering, Chengdu University of Information Technology, Chengdu 610225, PR China.

e. Research Institute of Frontier Science, Southwest Jiaotong University, Chengdu 610031, PR China.

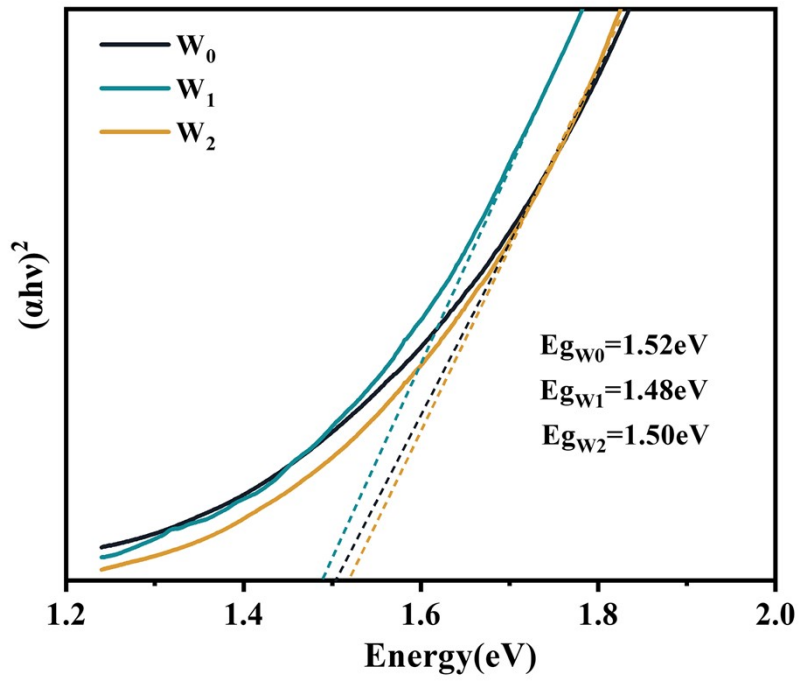
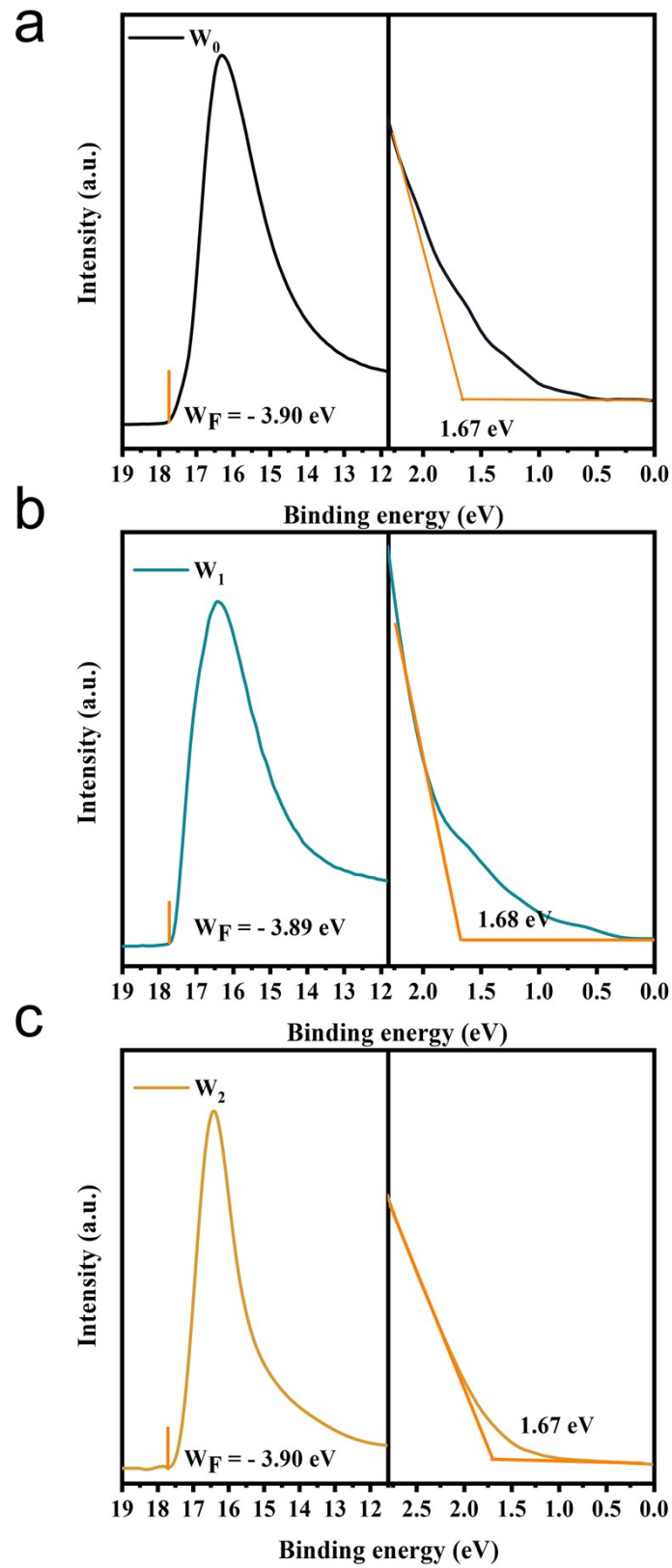
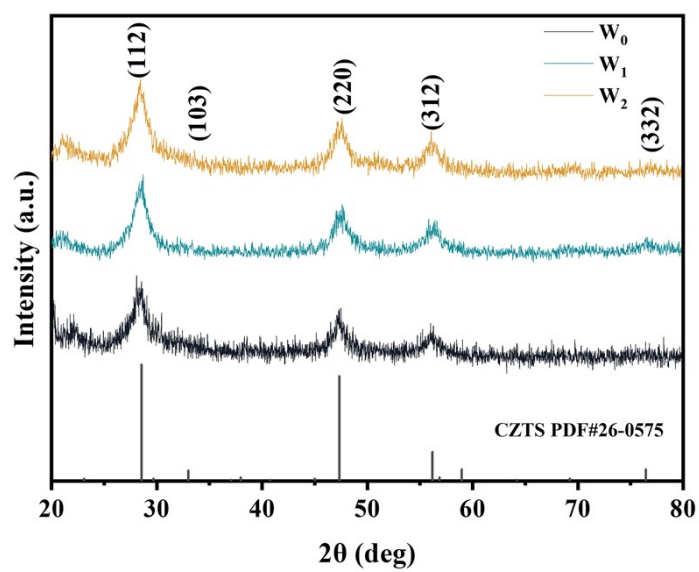


Figure S1. Bandgap spectra of  $W_0/W_1/W_2$  films.



**Figure S2.** a,b,c) UPS spectra of secondary electron cut-off and valence bands for  $W_0$  / $W_1$  / $W_2$  films.



**Figure S3.** XRD patterns of  $W_0/W_1/W_2$  films.

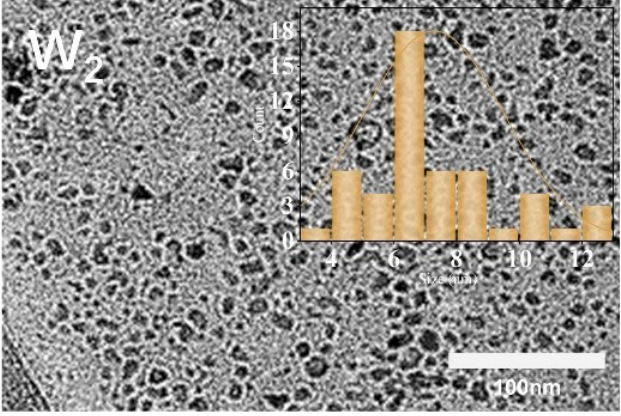
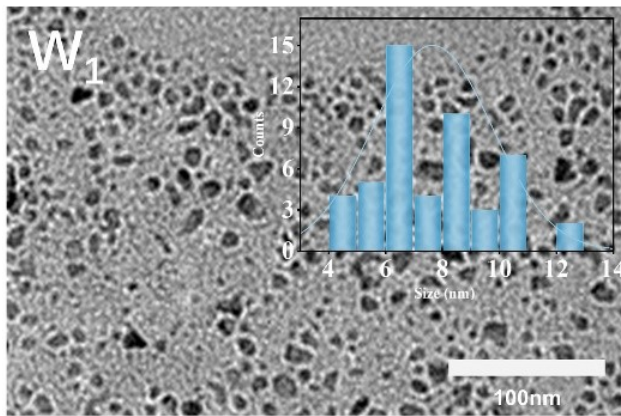
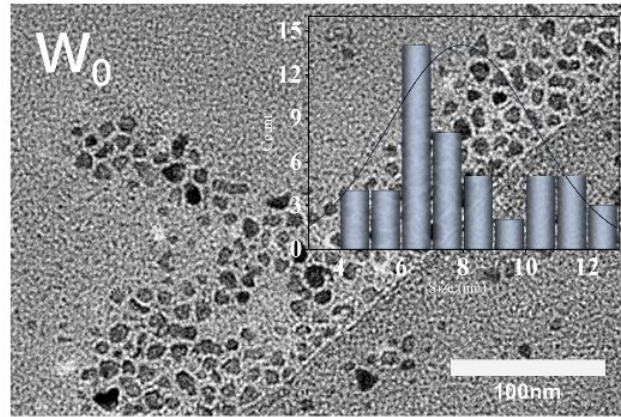


**Figure S4.** TEM image of  $W_0/W_1/W_2$  films.

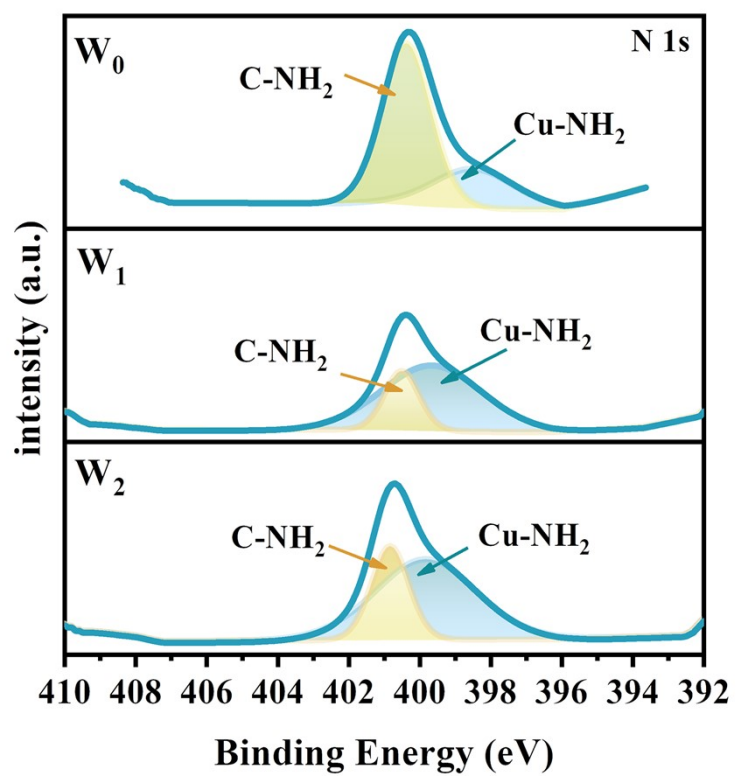


**Figure S5.** Deconvolution of N 1s core level from the XPS analysis of  $W_0/W_1/W_2$  films.

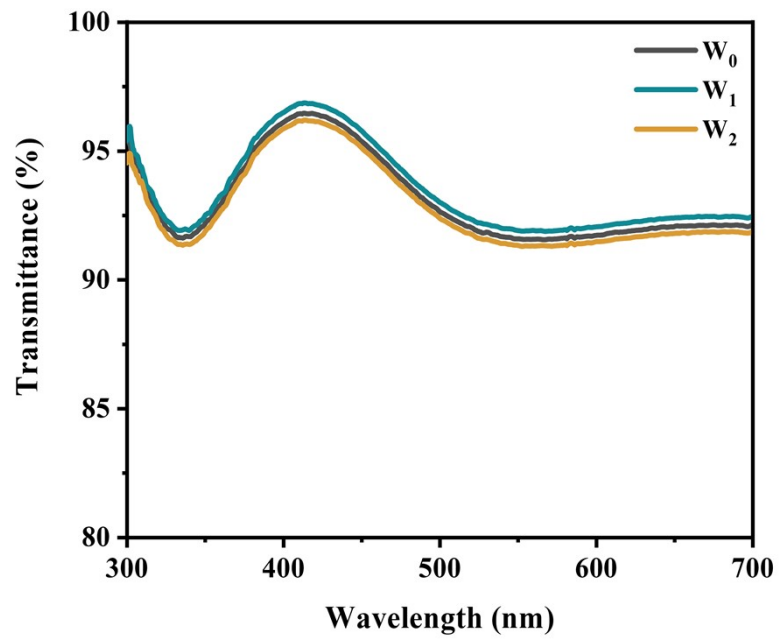
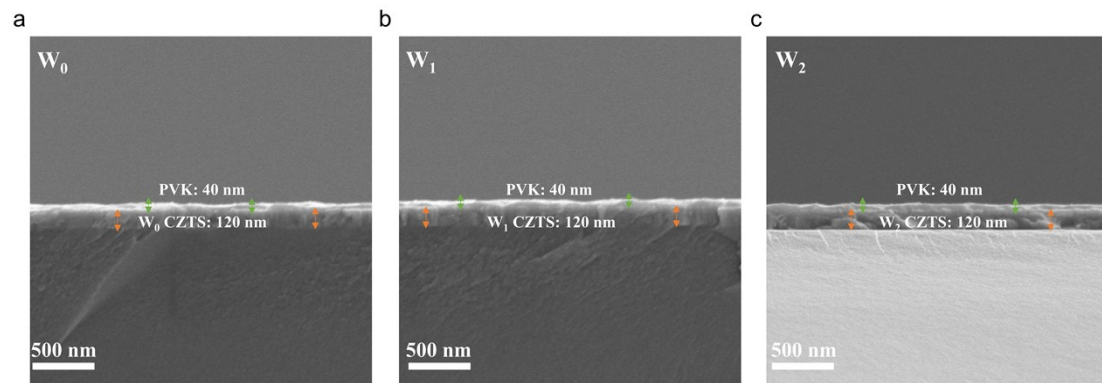
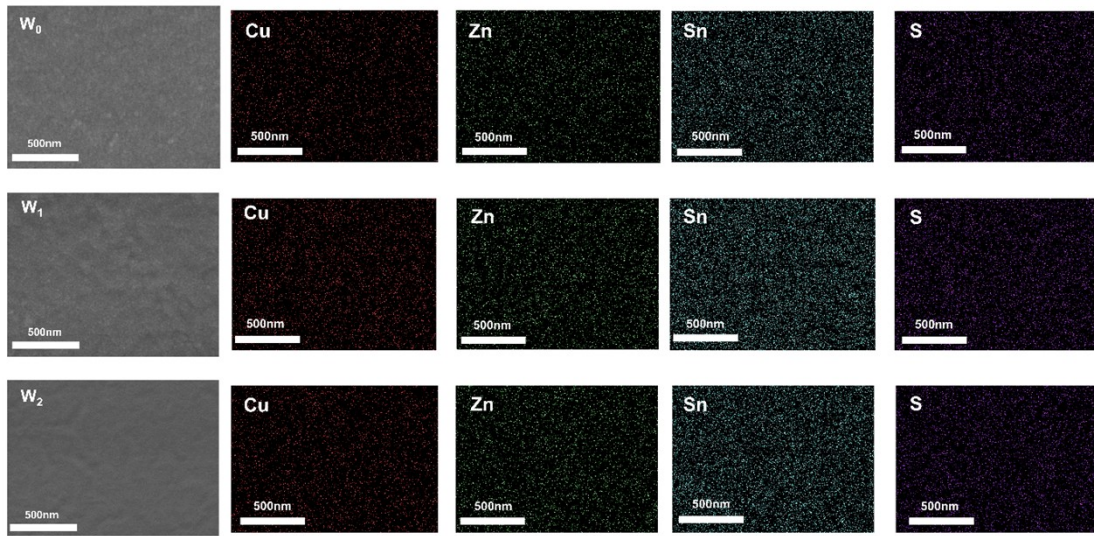


Figure S6. Transmittance spectra of  $W_0/W_1/W_2$  films.



**Figure S7.** Cross-section SEM images of perovskite films on W<sub>0</sub>/ W<sub>1</sub>/W<sub>2</sub> CZTS films.





**Figure S8.** The SEM images and EDS elemental mapping images and the concrete element contents of the  $W_0/W_1/W_2$  films.

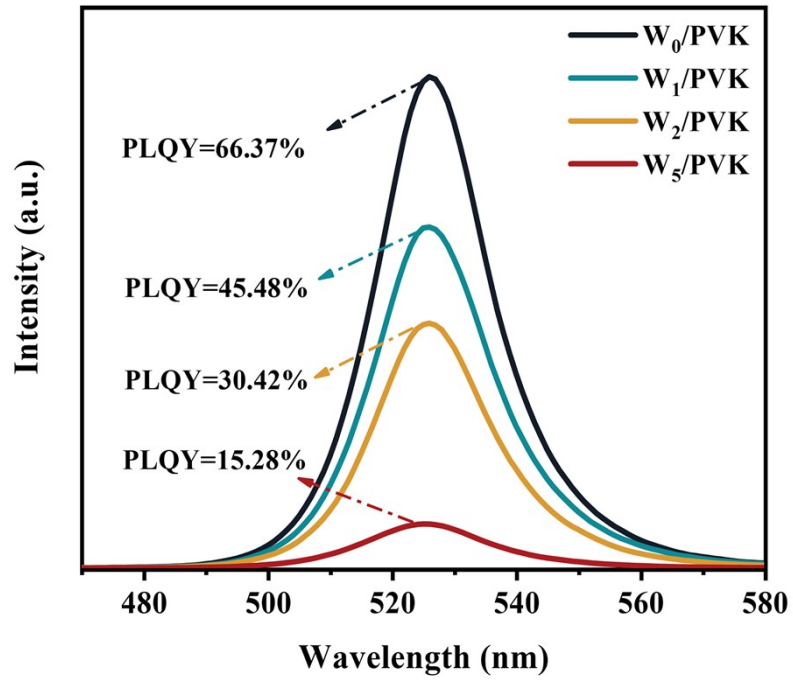


**Figure S9.** PLQY spectra of the perovskite film on  $W_0/W_1/W_2/W_5$  films.

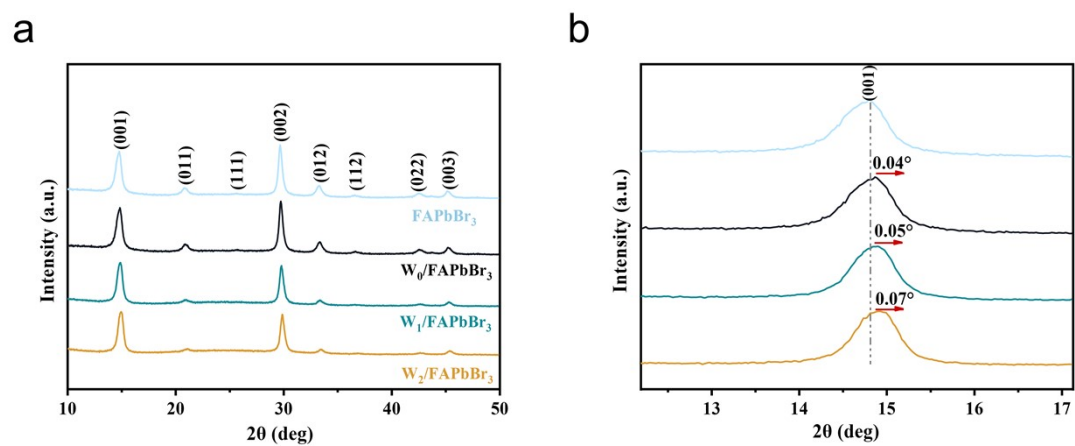


**Figure S10.** a) XRD patterns of perovskite films on W<sub>0</sub>/W<sub>1</sub>/W<sub>2</sub> films. b) Zoom out XRD peak from 12.5° to 17°.

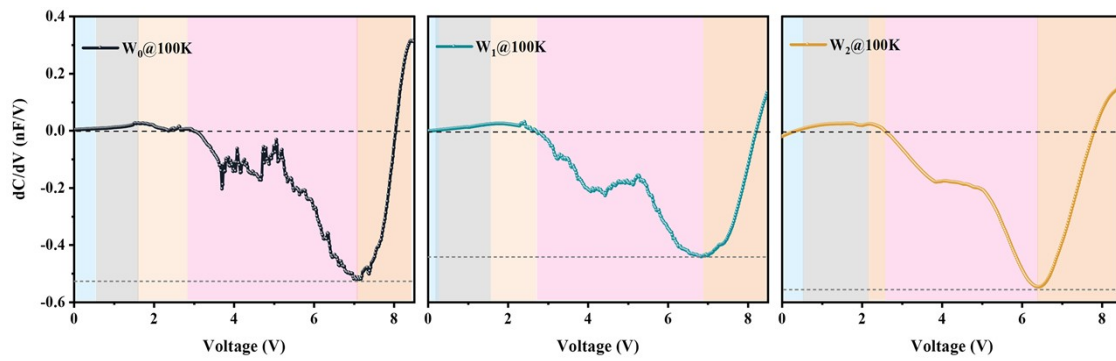


**Figure S11.**  $dC/dV$ - $V$  curves of  $W_0/W_1/W_2$ -based PeLEDs at frequency of 100K.

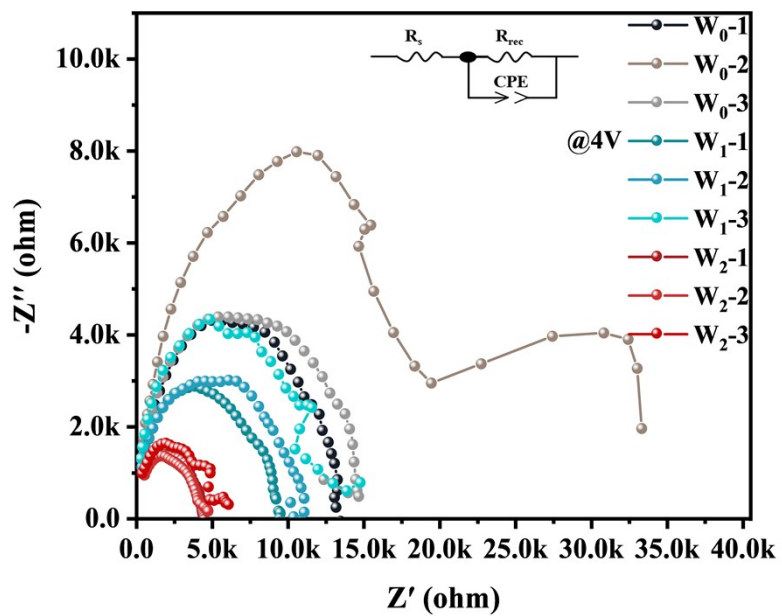


**Figure S12.** Nyquist plots of impedance spectra of  $W_0/W_1/W_2$ -based PeLEDs. Inset shows the equivalent circuit diagram for fitting.

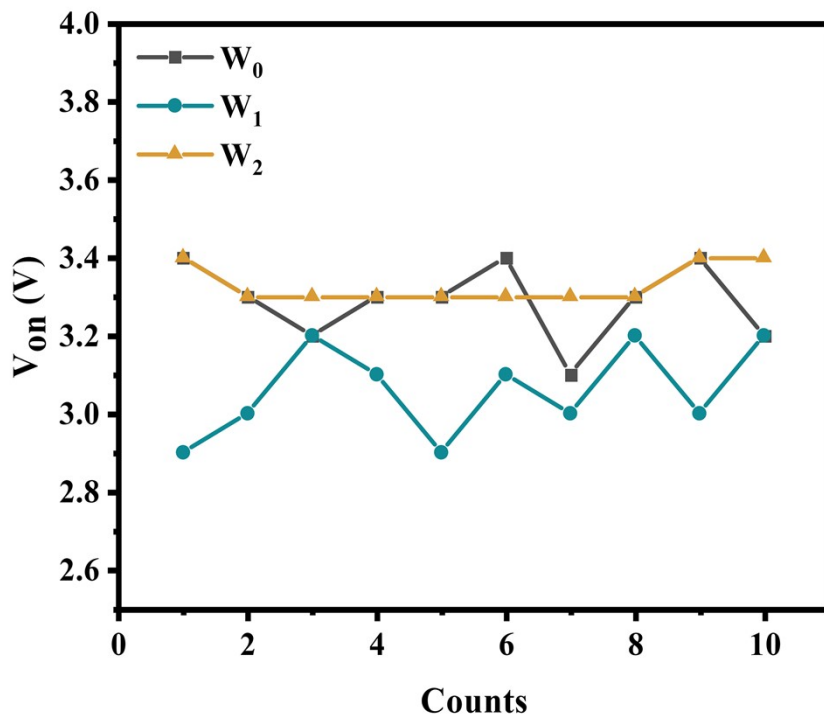
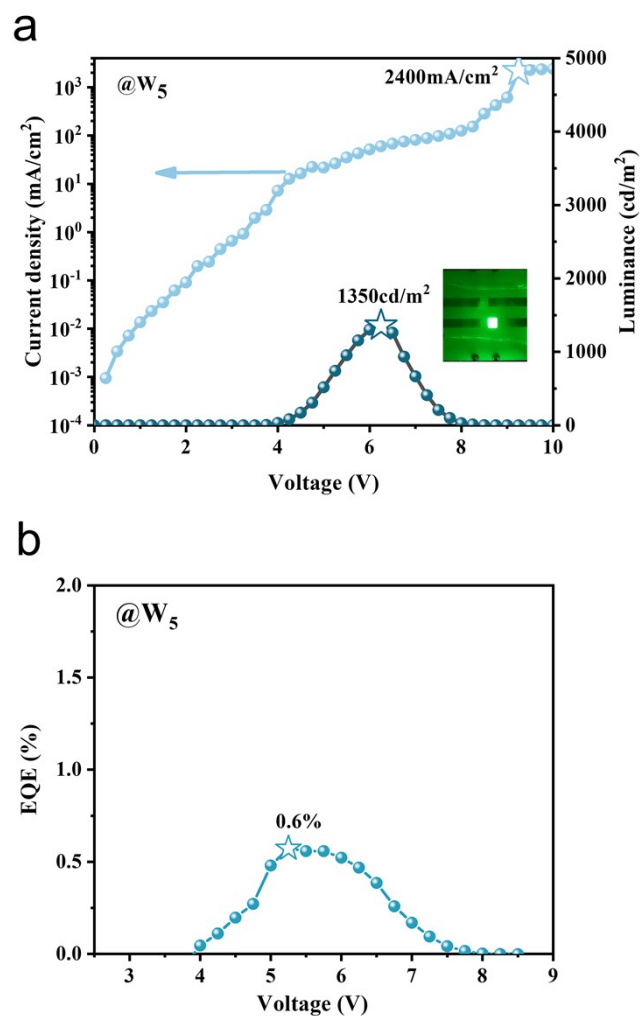
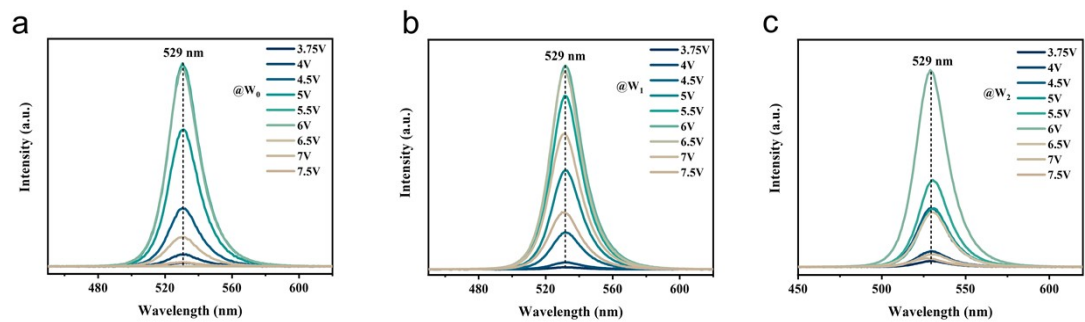


Figure S13. Statistical line chart of  $V_{on}$  for ten experiments of  $W_0/W_1/W_2$  devices.



**Figure S14.** a) Current density-luminance-voltage characteristics curves and b) EQE-voltage curves of  $W_5$ -based PeLEDs.



**Figure S15.** Variational EL spectra with increasing driven voltages of  $W_0$ / $W_1$ / $W_2$ -based PeLEDs.



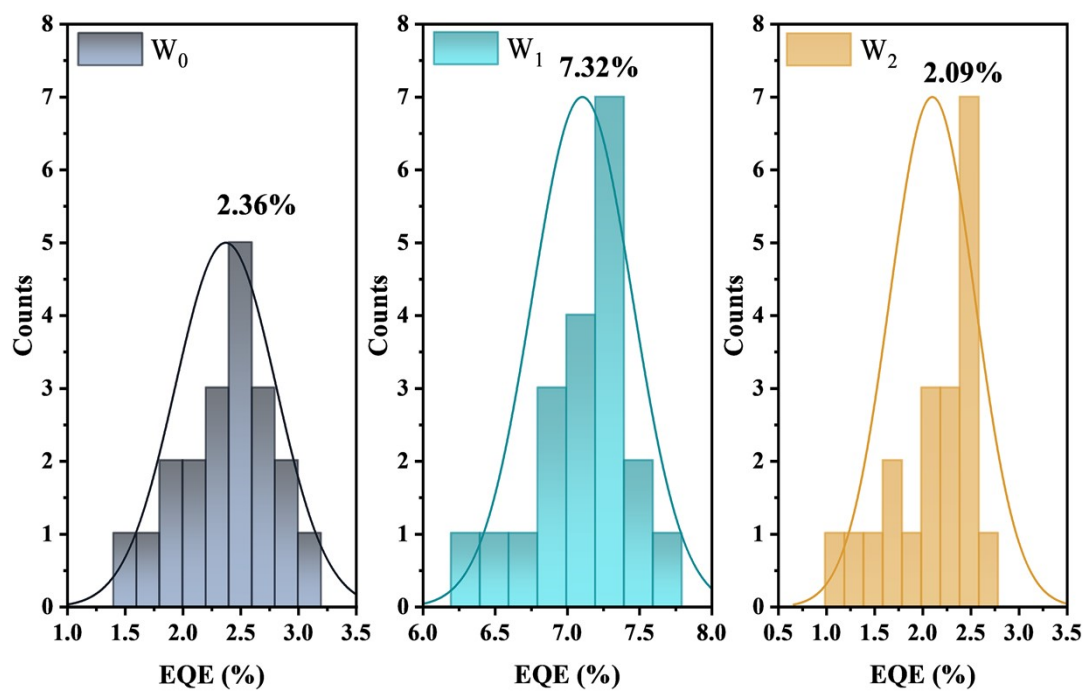


**Figure S16.** Statistic histogram of EQE of  $W_0/W_1/W_2$ -based PeLEDs.

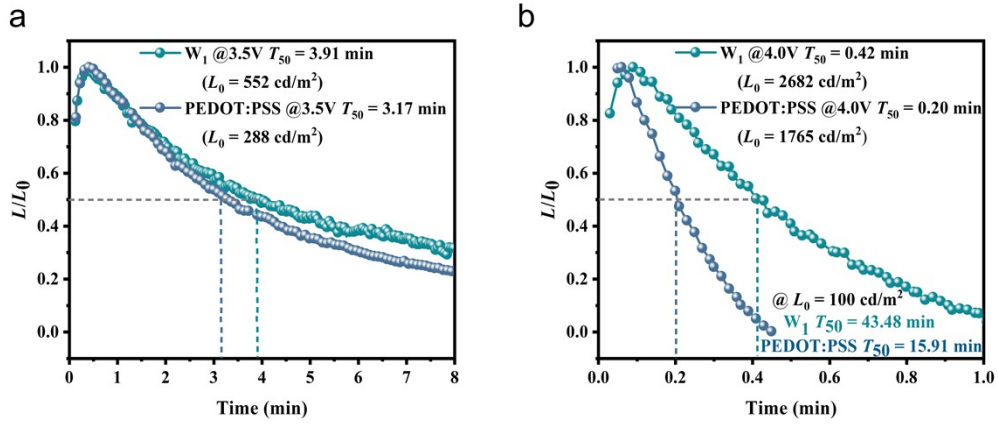


**Figure S17.**  $T_{50}$  measurements of PEDOT:PSS-based PeLEDs and CZTS-based PeLEDs at a) 3.5 V and b) 4.0 V.

**Table S1.** Fitting values of  $k_r$ ,  $k_{nr}$ ,  $\Gamma_{inh}$ ,  $\gamma_{AC}$ ,  $\gamma_{LO}$ , and  $E_{LO}$ ,  $E_B$  of perovskite films deposited on the  $W_0/W_1/W_2$  films.

Sample	$k_r$ ( $\times 10^7 \text{ s}^{-1}$ )	$k_{nr}$ ( $\times 10^7 \text{ s}^{-1}$ )	$\Gamma_{inh}$ (meV)	$\gamma_{AC}$ (eV/K)	$\gamma_{LO}$ (eV)	$E_{LO}$ (meV)	$E_B$ (meV)
$W_0$	3.73	1.91	50±3.34	$1.5 \times 10^{-4} \pm 3.2 \times 10^{-5}$	0.35±0.23	74.27±22.62	180.73±9.02
$W_1$	3.01	3.63	50±3.61	$1.3 \times 10^{-4} \pm 3.6 \times 10^{-5}$	0.35±0.16	66.93±16.03	169.16±8.08
$W_2$	2.70	6.20	50±6.7	$4.5 \times 10^{-5} \pm 8.1 \times 10^{-5}$	0.21±0.05	45.59±13.09	159.60±7.40